MRI and Luminescence Zn^{2+} Detection with a Lanthanide Complex–Zinc Finger Peptide Conjugate

Manon Isaac,[a] Agnès Pallier,[b] Frédéric Szeremeta,[b] Pierre-Alain Bayle,[c] Laurent Barantin,[d] Célia S. Bonnet*[b] and Olivier Sénèque*[a]

[a] Univ. Grenoble Alpes, CNRS, CEA, BIG, LCBM (UMR 5249), F-38000 Grenoble, France.

[b] Centre de Biophysique Moléculaire, UPR CNRS 4301, Université d'Orléans, rue Charles Sadron, F-45071 Orléans, France.

[c] Univ. Grenoble Alpes, CEA, INAC, MEM, F-38000 Grenoble, France.

[d] UMR 1253, iBrain, Université de Tours, Tours, France

Email: *olivier.seneque@cea.fr* and *celia.bonnet@cnrs.fr*

Supporting Information

Content

Abbreviations

PyBOP: (Benzotriazol-1-yloxy)tripyrrolidino-phosphonium-hexafluorophosphate; $Pd(PPh_3)_4$: *tetrakis*(triphenyl-phosphine)-palladium(0); TIS: triisopropylsilane; TCEP: *tris*(2-carboxyethyl)phosphine; DIEA: N,N-diisopropylethylamine; TFA: trifluoroacetic acid; MeCN: acetonitrile; DCM: dicholoromethane; Et_2O: diethylether; DMF: N,N-dimethylformamide; *t*Bu: *tert*-butyl; Trt: trityl; Fmoc: 9-fluorenylmethoxycarbonyl; Boc: tert-butyloxycarbobyl; Alloc: allyloxycarbonyl; HEDTA: N-hydroxyethyl-ethylenediamine-triacetic acid; HPLC: high performance liquid chromatography; ESI: electrospray ionization; MS: mass spectrometry; UV-Vis: ultraviolet-visible; CD: circular dichroism.

Materials and methods

Reagents and solvents: N-α-Fmoc-protected amino acids for peptide synthesis, PyBOP coupling reagent and NovaPEG Rink Amide resin were obtained from Novabiochem. DOTA-*tris*(tBu) ester was purchased from CheMatech. Other reagents for peptide synthesis, solvents, buffers and metal salts were purchased from Sigma-Aldrich. All buffer or metal solutions for spectroscopic measurements were prepared with MilliQ water (Millipore). The concentration of the Zn^{2+} solution was determined by colorimetric EDTA titrations.[1] Buffer solutions were treated with Chelex 100 resin (Biorad) to remove trace metal ions.

Analyses and purifications: Analytical HPLC separations were performed on an Agilent Infinity 1200 system using Merck PurospherStar RP-18e (150 mm × 4.6 mm) columns at 1 mL/min. Preparative HPLC separations were performed on a VWR LaPrepΣ system using a Waters XBridge Peptide BEH130 C18 (5 µm, 150 mm × 19 mm) column at 14 mL/min. Mobile phase consisted in a gradient of solvent A (0.1% TFA in H_2O) and B (0.1% TFA in MeCN/H_2O 9:1). For analytical separations, Method A consisted in 5% B during 2 min followed by a 5 to 80 % B gradient in 28 min. Eluate was monitored by electronic absorption at 214, 254 and 280. ESI-MS analyses were performed on a Thermo LXQ spectrometer. Induced Coupled Plasma Optical Emission Spectrometer (ICP-OES) measurements were performed in a Jobin Yvon ULTIMA2 Spectrometer. Both standards solutions and samples were prepared in 5% HNO_3. UV-Vis absorption spectra were recorded on a Perkin-Elmer Lambda 35 spectrophotometer.

Peptide synthesis

Synthesis of LZF2: Peptide elongation was performed on NovaPEG Rink Amide resin (0.40 mol g^{-1}; 0.1 mmol scale) using standard SPPS protocols using Fmoc/tBu chemistry on an automated peptide synthesizer (CEM Liberty1 Microwave Peptide Synthesizer) after attachment of the first amino acid by single manual coupling (30 min) using 2-fold excess of Fmoc-Gly-OH, 2-fold excess of PyBOP and 6-fold excess of DIEA in DMF followed by acetylation using (Ac_2O/pyridine/DMF 1:2:7 (by vol.), 10 mL, 5 min). For automated synthesis, double couplings (30 min) were performed using 4-fold molar excess of Fmoc-L-amino acid, 4-fold molar excess of PyBOP and 8-fold molar excess of DIEA at room temperature. A capping step was performed after each coupling with Ac_2O/DIEA in DMF (5 min). Fmoc removal was performed using 20% piperidine in DMF (2×10 min). After acetylation of the N-terminus, removal of the N-Alloc protecting group of the Lys(Alloc) residue was performed using with $Pd(PPh_3)_4$ (0.02 mmol, 23 mg) and phenylsilane (2.5 mmol, 0.3 mL) in degassed anhydrous DCM (15 mL) for 1 h in the dark.[2] The resin was then washed successively with DCM

(2×2 min), DMF (2×2 min), 1% H_2O in DMF (2×2 min), DMF (2×2 min), 1% DIEA in DMF (2×2 min), DMF (2×2 min), sodium diethyldithiocarbamate in DMF (0.12 M, 2×5 min) and DMF (2×2 min). DOTA-tris(*t*Bu) ester (0.2 mmol, 114 mg) was dissolved in a small amount of DMF and added to the resin, then a solution of PyBOP (0.2 mmol, 104 mg) and DIEA (0.6 mmol, 104 µL) in DMF (2 mL) was added. The resin was agitated overnight at room temperature, then washed with DMF (2×2 min), DCM (2×2 min) and Et_2O (2×2 min) and dried. Removal of acid-labile protecting groups and resin cleavage were performed using TFA/H_2O/TIS/thioanisole/DTT (18 mL:0.6 mL:0.6 mL:0.6 mL:300 mg) for 4 h. TFA was evaporated under reduced pressure and cold Et_2O was added to precipitate the peptide, which was purified by HPLC to give $LZF2^{Trp}$ (84 mg, 22% yield). HPLC (anal.) t_R = 13.7 min (method A); ESI-MS: average *m/z* = 1288.5 (3+), 966.7 (4+), 773.7 (5+), 644.8 (6+), 552.9 (7+) / calculated av. *m/z* = 1288.48 $[M+3H]^{3+}$, 966.61 $[M+4H]^{4+}$, 773.49 $[M+5H]^{5+}$, 644.74 $[M+6H]^{6+}$, 552.78 $[M+7H]^{7+}$ for M = $C_{171}H_{270}N_{48}O_{50}S_2$); deconvoluted mass found = 3863.3 / expected mass = 3862.41 (average isotopic composition).

Formation of Ln^{3+} complexes $LZF2^{Ln}$ (Ln = Tb or Gd): LZF2 (5 µmol, 20 mg) and $LnCl_3$ (50 µmol, 15 mg) were dissolved in H_2O and the pH was adjusted to 6.2 using NaOH. The solution was stirred overnight under argon (after 1h, the pH was controlled and adjusted to 6.2 if needed). TCEP (18 µmol, 5 mg) was added prior to removal of excess Ln^{3+} by HPLC purification. $LZF2^{Ln}$ was obtained as a white powder after freeze-drying (85-90% yield). **$LZF2^{Tb}$:** HPLC (anal.) t_R = 13.5 min (method A); ESI-MS: average *m/z* = 1340.5 (3+), 1005.7 (4+), 804.8 (5+), 670.9 (6+), 575.2 (7+) / calculated av. *m/z* = 1340.44 $[M+3H]^{3+}$, 1005.58 $[M+4H]^{4+}$, 804.67 $[M+5H]^{5+}$, 670.73 $[M+6H]^{6+}$, 575.05 $[M+7H]^{7+}$ for M = $C_{171}H_{267}N_{48}O_{50}S_2Tb$); deconvoluted mass found = 4019.2 / expected mass = 4018.30 (average isotopic composition). **$LZF2^{Gd}$:** HPLC (anal.) t_R = 13.7 min (method A); ESI-MS: average *m/z* = 1340.0 (3+), 1005.3 (4+), 804.4 (5+), 670.6 (6+), 575.0 (7+) / calculated av. *m/z* = 1339.89 $[M+3H]^{3+}$, 1005.17 $[M+4H]^{4+}$, 804.33 $[M+5H]^{5+}$, 670.45 $[M+6H]^{6+}$, 574.82 $[M+7H]^{7+}$ for M = $C_{171}H_{267}N_{48}O_{50}S_2Gd$); deconvoluted mass found = 4016.9 / expected mass = 4016.63 (average isotopic composition).

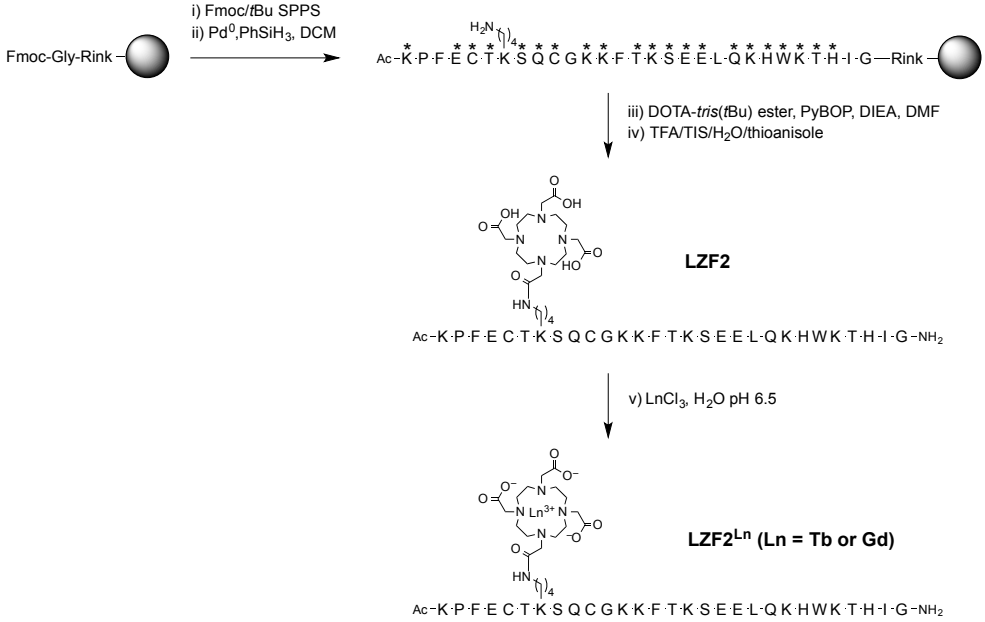

Figure S1. Synthetic pathway for the preparation of $LZF2^{Ln}$ (Ln = Tb or Gd). * denotes a standard side chain protecting group (Boc for Lys and Trp; *t*Bu for Glu, Thr and Ser; Trt for Cys, Gln and His).

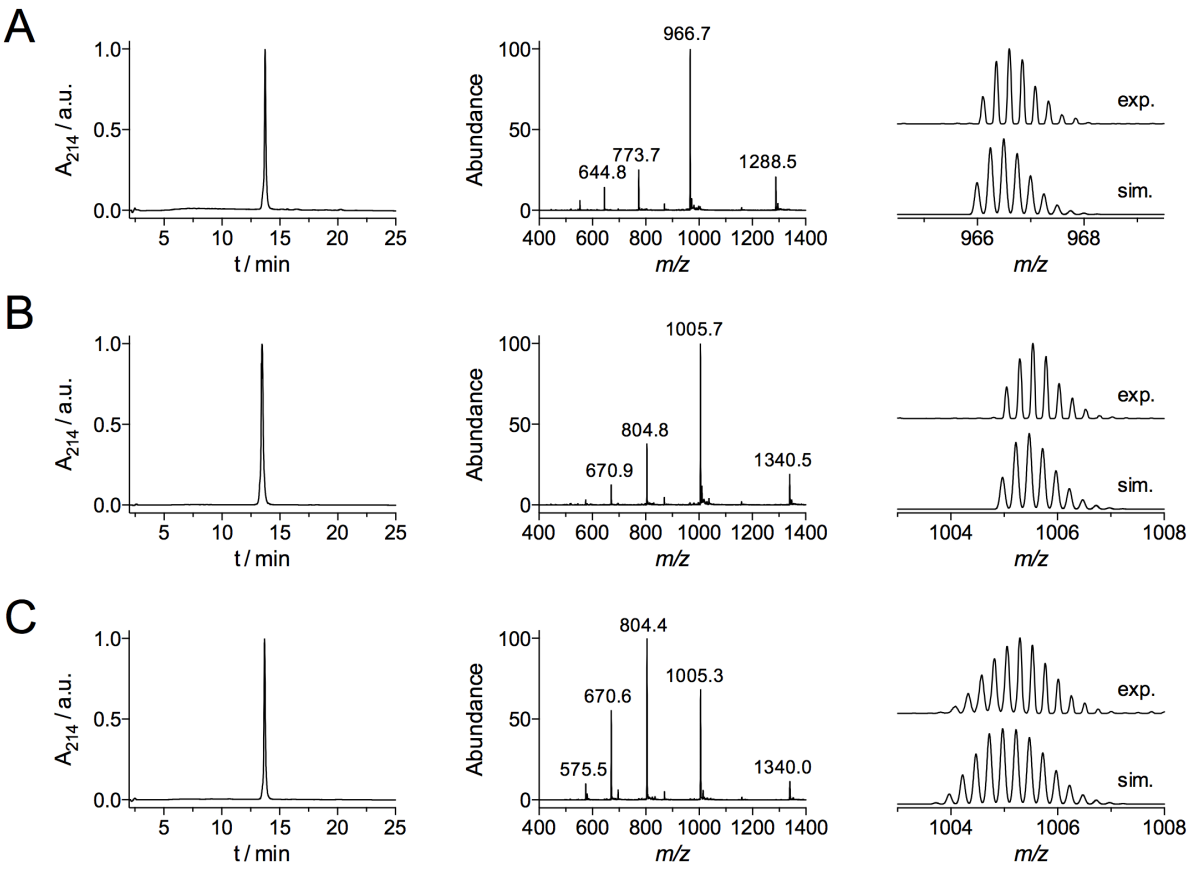

Figure S2. HPLC chromatograms (*left*) and ESI-MS spectra (*middle*: full MS spectrum; *right*: experimental and simulated isotopic pattern of the $[M+4H]^{4+}$ peak) of (A) LZF2, (B) $LZF2^{Tb}$ and (C) $LZF2^{Gd}$.

Circular dichroism

Sample preparation and measurements: Circular dichroism was used to monitor the Zn-induced folding of $LZF2^{Tb}$. For this purpose a solution of $LZF2^{Tb}$ (5.5 µM) was prepared in an aerated phosphate buffer (10 mM, pH 7.5) containing TCEP (250 µM) as a reducing agent. The concentration of $LZF2^{Tb}$ was estimated using the extinction coefficients of tryptophan (ε = 5690 M^{-1} cm^{-1} at 280 nm). Zn^{2+} was titrated into this solution using a $Zn(ClO_4)_2$ solution (1.68 mM in water). CD spectra were recorded on an Applied Photophysics Chirascan spectropolarimeter equipped with a thermo-regulated cell holder using 0.4 cm path length cuvettes. Spectra were recorded from 300 nm to 200 nm every 1 nm with a 2 s signal averaging for each point. Each spectrum was recorded twice, averaged and smoothed using a Stavitsky-Golay filter.

Luminescence spectroscopy

Measurements: All measurements were performed using aerated solutions. Emission and excitation spectra and Tb^{3+} luminescence lifetimes were measured on a Varian Cary Eclipse spectrometer equipped with a thermo-regulated cell holder. Time-resolved Tb^{3+} luminescence spectra were acquired with 100 µs time delay.

Sample preparation and Zn^{2+} titrations: All samples were prepared in a HEPES buffer (10 mM, pH 7.5) containing TCEP (250 µM) as a reducing agent. Typically, the concentration of $LZF2^{Tb}$ was 5-10 µM as

determined using the extinction coefficient of tryptophan at 280 nm (ε = 5690 M^{-1} cm^{-1}). Zn^{2+} titrations were performed using a $Zn(ClO_4)_2$ solution (1.68 mM in water). For selectivity experiments, stock solutions of perchlorate salts (2 mM for Mn^{2+}, Fe^{2+}, Co^{2+}, Ni^{2+} and Cu^{2+}, 100 mM for Ca^{2+} and Mg^{2+} and 1 M for Na^+ and K^+ in water, depending on the cation used) were used. Samples contained 2 eq. of Mn^{2+}, Fe^{2+}, Co^{2+}, Ni^{2+} and Cu^{2+} *vs* LZF2. For alkali and alkaline earth cations, concentration of Na^+ or K^+ in solutions was 50 mM and that of Ca^{2+} or Mg^{2+} was 10 mM).

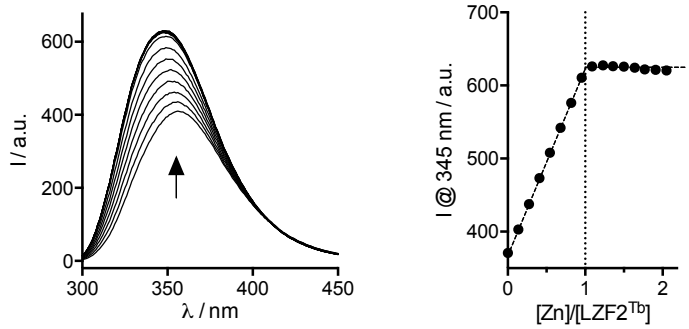

Figure S3. Evolution of the tryptophan fluorescence emission (λ_{ex} = 280 nm) upon addition of Zn^{2+} in a solution of $LZF2^{Tb}$ (9 µM) in a HEPES buffer (10 mM, pH 7.5, 250 µM TCEP).

Determination of *q*, the number of water molecules coordinated to Tb^{3+}: Solutions of $LZF2^{Tb}$ in a HEPES buffer (10 mM, pH 7.5) containing TCEP (250 µM) were prepared in various H_2O/D_2O mixtures (25, 50, 75 and 100 % H_2O). Lifetimes in 100 % D_2O were extrapolated from the plot of the rate constants of Tb^{3+} luminescence decay ($k_{Ln} = \tau_{Ln}^{-1}$) against the fraction of H_2O in H_2O/D_2O mixtures (Figure S4). The number of water molecules coordinated to the Tb^{3+} ion (q) was determined using $q = 5\times(k_{Tb/H2O} - k_{Tb/D2O} - 0.06)$.[3] Table S1 summarizes lifetimes and q values.

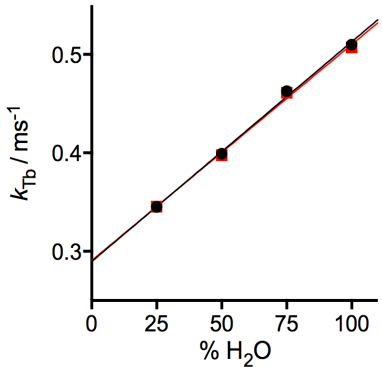

Figure S4. Plot of the Tb^{3+} luminescence decay rate constants k_{Tb} against the volume fraction of H_2O in H_2O/D_2O mixtures for free (black) and Zn-loaded (red) $LZF2^{Tb}$. Decays were recorded in a HEPES buffer (10 mM, pH 7.5).

Table S1. Luminescence data for free and Zn-loaded LZF2 probes (10 µM) in HEPES buffer (10 mM, pH 7.5).

Compounds	τ_{Ln} in H_2O	τ_{Ln} in D_2O	q (± 0.3)
$LZF2^{Tb}$	1.96 (1) ms	3.45 (1) ms	0.8
$Zn{\cdot}LZF2^{Tb}$	1.97 (1) ms	3.44 (1) ms	0.8

Determination of the Zn^{2+} binding constant

The binding constant of Zn^{2+} to $LZF2^{Tb}$ was determined by titrating a solution containing the $LZF2^{Tb}$ probe and a known amount of an appropriate competitor tested among EDTA, HEDTA and EGTA in HEPES buffer (10 mM, pH 7.5, TCEP 250 µM). Time-resolved Tb^{3+} emission was used to monitor the titration. EDTA and EGTA were found to be too strong and too weak competitors, respectively, and the binding constant was determined using HEDTA. The evolution of the intensity against the Zn^{2+}/peptide ratio (r) was fitted to the equilibrium $Zn{\cdot}LZF2^{Tb}$ + HEDTA ⇌ $LZF2^{Tb}$ + Zn·HEDTA by Equations (1-7) in which I_0 and I_F are the emission intensities at the beginning and the end of the titration, $[LZF2^{Tb}]_t$, $[HEDTA]_t$ and $[Zn]_t$ the total concentrations of $LZF2^{Tb}$, HEDTA and Zn^{2+} introduced in the solution. The apparent Zn^{2+} binding constant of HEDTA at pH 7.5 was calculated from pK_a and log β_{11} values reported in the literature: $K_{ZnHEDTA} = 10^{12.1}$.[4,5] The dilution could be neglected. Figure S5 shows the Zn^{2+} titrations of $LZF2^{Tb}$ in the presence of HEDTA and its fit, which yielded $K_{ZnLZF2}/K_{ZnHEDTA} = 0.43 \pm 0.04$.

$$I = I_0 + \frac{I_F - I_0}{[LZF2^{Tb}]_t} \times \frac{-b - \sqrt{b^2 - 4ac}}{2a} \quad \text{when } [Zn]_t < [LZF2^{Tb}]_t + [HEDTA]_t \tag{1}$$

$$I = I_F, \text{ when } [Zn]_t > [LZF2^{Tb}]_t + [HEDTA]_t \tag{2}$$

$$r = \frac{[Zn]_t}{[LZF2^{Tb}]_t} \tag{3}$$

$$a = K - 1 \tag{4}$$

$$b = r[LZF2^{Tb}]_t - [HEDTA]_t - rK[LZF2^{Tb}]_t - K[LZF2^{Tb}]_t \tag{5}$$

$$c = rK[LZF2^{Tb}]_t^2 \tag{6}$$

$$K = \frac{K_{ZnLZF2Tb}}{K_{ZnHEDTA}} \tag{7}$$

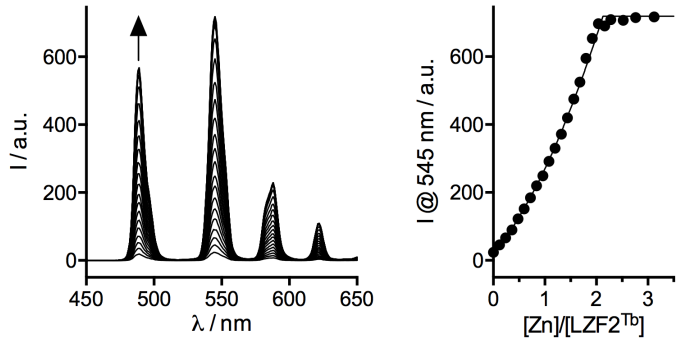

Figure S5. Evolution of the time-resolved Tb^{3+} emission (λ_{ex} = 280 nm) upon addition of Zn^{2+} in a solution of $LZF2^{Tb}$ (7 µM) in a HEPES buffer (10 mM, pH 7.5, 250 µM TCEP) containing HEDTA (7.9 µM) as a competitor. The solid line on the right panel corresponds to the fit to the equilibrium $Zn{\cdot}LZF2^{Tb}$ + HEDTA ⇌ $LZF2^{Tb}$ + Zn·HEDTA by Equations (1-7).

Relaxometric studies

NMRD Profiles: All measurements were performed on a Stelar SMARTracer Fast Field Cycling relaxometer (0.01-10 MHz) and a Bruker WP80 NMR electromagnet adapted to variable field measurements (20-80 MHz) and controlled by a SMARTracer PC-NMR console. The temperature was monitored by a VTC91 temperature control unit and maintained by a gas flow. The temperature was determined by previous calibration with a Pt resistance temperature probe. The longitudinal relaxation rates ($1/T_1$) were determined in water. At 200 and 400 MHz, $1/T_1$ measurements were performed in a capillary tube placed in a 5 mm tube containing D_2O using the inversion recovery sequence on a Bruker Avance DMX (200 MHz) equipped with a 5 mm BBIZ probe and a Bruker Avance III (400 MHz) equipped with a 5 mm BBO SmartProbe, respectively. The least-squares fit of the ^{1}H NMRD data were performed using Visualiseur/Optimiseur[6,7] running on a MATLAB 8.3.0 (R2014a) platform using equations derived below. In the fitting procedure, we have fixed the r_{GdO} distance to 2.50 Å, based on available crystal structure and ENDOR results, the r_{GdH} distance to 3.10 Å and the closest approach of the bulk water protons to the Gd^{3+}, a_{GdH} to 3.5 Å.[8] The quadrupolar coupling constant, $\chi(1+\eta^{2/3})^{1/2}$, has been set to the value for pure water, 7.58 MHz.[9] The diffusion constant has been fixed to 26×10^{-10} m^2 s^{-1} and its activation energy to 10 kJ mol^{-1}. The hydration number was 1 as determined by luminescence lifetime measurements on the Tb^{3+} analogue. The water exchange rate and the water exchange enthalpy were fixed to the values obtained for GdDOTAMA systems ($k_{ex}^{298} = 1.6\times10^{-6}$ s^{-1} and $\Delta H^{\neq} = 40$ kJ mol^{-1}).[10] The activation energy of the correlation time for the modulation of the zero-field splitting E_V has been fixed to 1 kJ.mol^{-1}. The fitting has been restricted to frequencies above 4.5 MHz as at low magnetic fields the SBM theory fails in describing electronic parameters and rotational dynamics of slowly rotating objects.

Table S2. Best-fit parameters obtained from the fitting of the ^{1}H NMRD profiles to the SBM theory, including the Lipari-Szabo approach for internal flexibility.

Parameters	$LZF2^{Gd}$	$Zn{\cdot}LZF2^{Gd}$
q^a	1	1
k_{ex}^{298} (10^6 s^{-1})^a	1.6	1.6
$\Delta H^{\neq}$ (kJ mol^{-1})^a	40	40
E_l (kJ mol^{-1})	46 ± 6	20 ± 14
τ_l^{298} (ps)	330 ± 30	145 ± 40
E_g (kJ mol^{-1})	23 ± 2	13 ± 2
τ_g^{298} (ps)	900 ± 50	1160 ± 60
S^2	0.48 ± 0.05	0.64 ± 0.04
E_V (kJ mol^{-1})^a	1	1
τ_V^{298} (ps)	16 ± 2	25 ± 3
Δ^2 (10^{19} s^{-2})	0.062 ± 0.003	0.051 ± 0.002

^{a} Fixed during the fitting procedure.

Sample preparation: All samples were prepared in a HEPES buffer (100 mM, pH 7.4) containing TCEP (28 μM) as a reducing agent. The concentration of $LZF2^{Gd}$ was determined using the extinction coefficient of tryptophan at 280 nm (ε = 5690 M^{-1} cm^{-1}) and the concentrations of Gd^{3+}-containing solutions were systematically checked by ICP-OES. Samples were degassed with N_2 before measurements. For Zn^{2+} titrations (Figure S6A), ^{1}H relaxivity measurements were performed at 20 MHz and 37°C with [$LZF2^{Gd}$] = 0.65 mM after

addition of a $ZnSO_4$ solution. To assess the influence of alkali or alkaline earth (Figure S6B), ^1H relaxivity measurements were performed at 20 MHz and 37°C with [$LZF2^{Gd}$] = 0.70 mM before and after addition of a solution of cation (Na^+, K^+, Mg^{2+} or Ca^{2+}, 1.0 eq. *vs* $LZF2^{Gd}$) and then after further addition of Zn^{2+} (1.5 eq.).

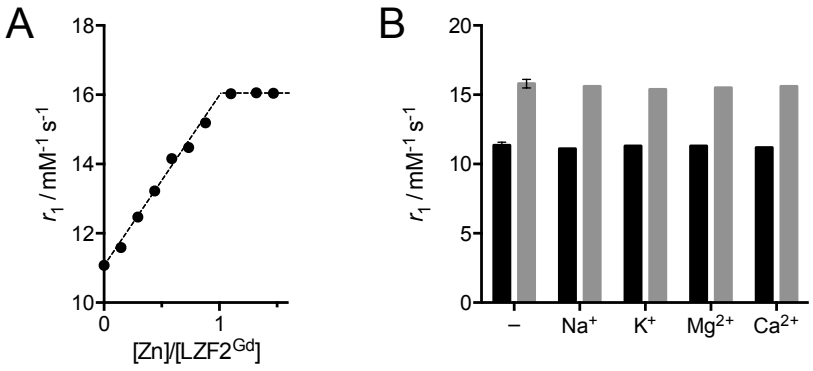

Figure S6. (A) ^1H relaxivity measurements (20 MHz, 37°C) in the presence of $LZF2^{Gd}$ (0.65 mM) in a HEPES buffer solution (100 mM, pH 7.4, 28 mM TCEP) with increasing amount of Zn^{2+} at 20 MHz and 37°C. (B) Selectivity diagram showing relaxivity (20 MHz, 37°C) of a solutions of $LZF2^{Gd}$ (0.70 mM) in a HEPES buffer (100 mM, pH 7.4, 28 mM TCEP) in the absence or presence of Na^+, K^+, Mg^{2+} or Ca^{2+} (0.7 mM, 1 eq.), before (grey) or after (black) addition of Zn^{2+} (1.5 eq.).

Temperature dependent ^{17}O NMR measurements

The transverse ^{17}O relaxation rates ($1/T_2$) were measured in aqueous solutions of [$LZF2^{Gd}$] = 1.14 mM, pH 7.5 or [$Zn{\cdot}LZF2^{Gd}$] = 1.36 mM, pH 7.4 in the temperature range 274-318 K, Bruker Nanobay 400 (9.4 T, 54.5 MHz) spectrometer. The temperature was calculated according to previous calibration with ethylene glycol and methanol.[11] An acidified water solution ($HClO_4$, pH 3.3) was used as external reference. Transverse relaxation times (T_2) were obtained by the Carr-Purcell-Meiboom-Gill spin-echo technique.[12] The technique of the ^{17}O NMR measurements on Gd^{3+} complexes has been described elsewhere.[13] The samples were sealed in glass spheres fitted into 10 mm NMR tubes to avoid susceptibility corrections of the chemical shifts.[14] To improve the sensitivity, ^{17}O-enriched water (10% $H_2{}^{17}O$, CortectNet) was added to the solutions to reach around 1% enrichment.

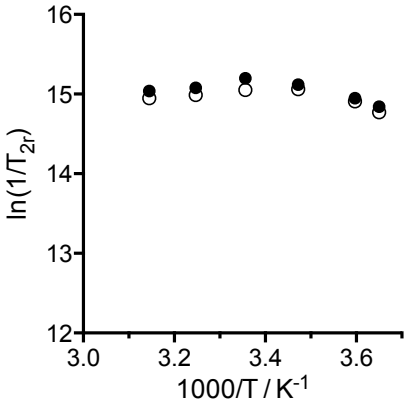

Figure S7. Temperature dependence of reduced ^{17}O transverse relaxation rates of $LZF2^{Gd}$ (1.14 mM, ○) and $Zn{\cdot}LZF2^{Gd}$ (1.36 mM, ●) at 9.4 T.

MRI images:

1.5 T images: All acquisitions were performed on a 1.5T clinical scanner (Siemens Aera) using a 20 elements head/neck coil. Acquisitions of a single slice (4mm thickness, in-plane resolution 0.72x0.72mm) were performed using single echo spin echo sequences with short echo time (TE = 8.4 ms) and variable repetition times (TR= 50, 100, 150, 200, 250, 300, 500 and 1000 ms). Samples were placed in a water bath maintained at 37°C. The T_1 relaxation time of each phantom was calculated, using a mono-exponential fitting, from signal mean intensity measured on the images as a function of TR, from figure S8. $LZF2^{Gd}$ and Zn-loaded $LZF2^{Gd}$ have T_1 values of respectively 435 ms, and 307 ms. This corresponds to a *ca.* 40 % increase, in accordance with NMRD measurements.

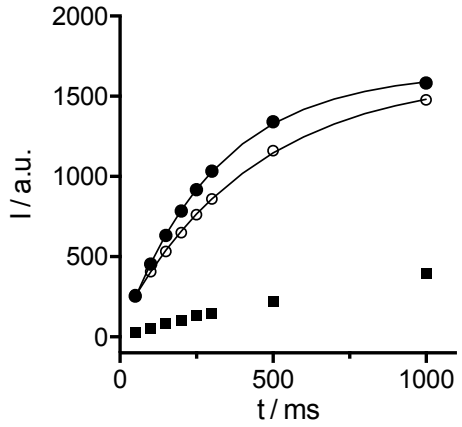

Figure S8. Mean intensity of phantoms of $LZF2^{Gd}$ (○), Zn-loaded $LZF2^{Gd}$ (●) and HEPES (■) measured on MRI images acquired with a fixed TE value of 8.4 ms and with 8 different TR values ranging from 50 ms to 1000 ms. Images were acquired with a spin echo sequence on a clinical scanner (Siemens Aera, 1.5 T). A mono-exponential fitting of these curves allows measurement of the T_1 relaxation time constants of the samples.

9.4 T images: Phantoms of $LZF2^{Gd}$, Zn-loaded $LZF2^{Gd}$ and HEPES have been imaged together with a classical Bruker birdcage coil, 35 mm inner diameter, on a BioSpec 9.4 T spectrometer (Bruker, Wissembourg, France). A spin echo sequence was used, to acquire images of each sample with a fixed TE of 9.92 ms and a variable TR ranging from 50 ms to 3000 ms. Using ISA-Tool program, provided with Paravision 5.1, the T_1 relaxation time of each phantom was calculated, using an exponential fitting, from signal mean intensity measured on the images as function of TR. Background mean intensity, referred to as noise, was also measured. Figure S9 shows the measured mean intensities as function of TR. As noise remains constant, ISA-Tool gives good T_1 estimation. $LZF2^{Gd}$ and Zn-loaded $LZF2^{Gd}$ and HEPES have T_1 values of 870 ms, 970 ms, and 2660 ms, respectively.

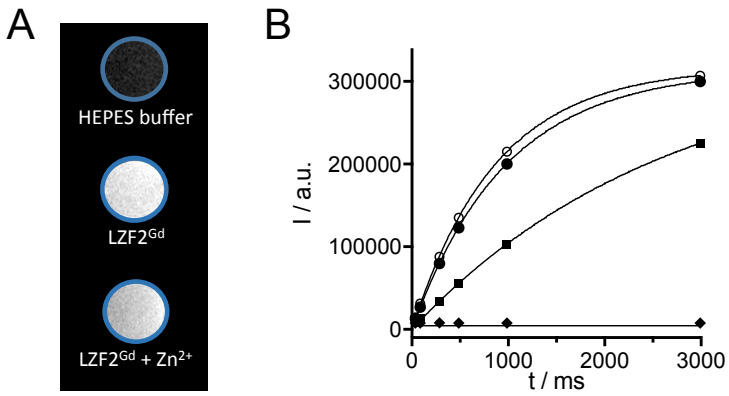

Figure S9. (A) T_1-weighted MR images of phantoms containing LZF2Gd (166 μM) in the absence (T_1 = 870 ms) or in the presence (T_1 = 970 ms) of 1.5 eq of Zn^{2+}, in a HEPES buffer (0.1 M, pH = 7.4) containing TCEP (30 mM). Images were acquired at 9.4 T using spin echo sequence with TE = 9.92 ms, TR = 500 ms. T_1 were measured with TE = 9.92 ms and variable TR from 50 to 3000 ms. (B) Mean intensity of phantoms of $LZF2^{Gd}$ (○), Zn-loaded $LZF2^{Gd}$ (●) and HEPES (■), and of background noise (◆) measured on MRI images acquired at a fixed TE value of 9.92 ms, with 6 different TR values ranging from 50 ms to 3000 ms. Images were acquired with a spin echo sequence at 9.4 T, with a BioSpec 94/20 Bruker spectrometer. An exponential fitting of these curves allows measurement of the T1 relaxation time constants of the phantoms.

Equations used for the fitting of NMRD data, with the SBM model including the model-free Lipari-Szabo approach

The measured longitudinal proton relaxation rate, $R_1^{obs} = 1/T_1^{obs}$, is the sum of a paramagnetic and a diamagnetic contribution as expressed in Equation (8), where r_1 is the proton relaxivity:

$$R_1^{obs} = R_1^d + R_1^p = R_1^d + r_1[\mathrm{Gd}^{3+}] \tag{8}$$

The relaxivity can be divided into an inner and an outer sphere term as follows:

$$r_1 = r_{1is} + r_{1os} \tag{9}$$

The inner sphere term is given in Equation (10), where q is the number of inner sphere water molecules.[15]

$$r_{1is} = \frac{1}{1000} \times \frac{q}{55.55} \times \frac{1}{T_{1m}^H + \tau_m} \tag{10}$$

The longitudinal relaxation rate of inner sphere protons, $1/T_{1m}^H$ is expressed by Equation (11), where r_{GdH} is the effective distance between the electron charge and the ^{1}H nucleus, ω_I is the proton resonance frequency and ω_S is the Larmor frequency of the Gd^{3+} electron spin.

$$\frac{1}{T_{1m}^H} = \frac{2}{15}\left(\frac{\mu_0}{4\pi}\right)^2 \frac{\hbar^2 \gamma_I^2 \gamma_S^2}{r_{GdH}^6} S(S+1) \times \left[3J(\omega_I;\tau_{d1}) + 7J(\omega_S;\tau_{d2})\right] \tag{11}$$

$$\frac{1}{\tau_{di}} = \frac{1}{\tau_m} + \frac{1}{\tau_{RH}} + \frac{1}{T_{ie}} \qquad \text{for } i = 1, 2 \tag{12}$$

where τ_{RH} is the rotational correlation time of the Gd-H_{water} vector.

For small molecular weight chelates (fast rotation), the spectral density function is expressed as in Equation (13).

$$J(\omega;\tau\ )=\left(\frac{\tau}{1+\omega^2\tau^2}\right) \tag{13}$$

For slowly rotating species, the spectral density functions are described the Lipari-Szabo approach.[16] In this model we distinguish two statistically independent motions; a rapid local motion with a correlation time τ_l and a slower global motion with a correlation time τ_g. Supposing the global molecular reorientation is isotropic, the relevant spectral density functions are expressed as in Equations (14-18), where the general order parameter S^2 describes the degree of spatial restriction of the local motion. If the local motion is isotropic, $S^2 = 0$; if the rotational dynamics is only governed by the global motion, $S^2 = 1$.

$$J(\omega_I;\tau_{d1})=\left(\frac{S^2\tau_{d1g}}{1+\omega_I^2\tau_{d1g}^2}+\frac{(1-S^2)\tau_{d1}}{1+\omega_I^2\tau_{d1}^2}\right) \tag{14}$$

$$J(\omega_S;\tau_{d2})=\left(\frac{S^2\tau_{d2g}}{1+\omega_S^2\tau_{d2g}^2}+\frac{(1-S^2)\tau_{d2}}{1+\omega_S^2\tau_{d2}^2}\right) \tag{15}$$

$$\frac{1}{\tau_{dig}}=\frac{1}{\tau_m}+\frac{1}{\tau_g}+\frac{1}{T_{ie}} \qquad i=1,2 \tag{16}$$

$$\frac{1}{\tau}=\frac{1}{\tau_g}+\frac{1}{\tau_l} \tag{17}$$

$$J_i(\omega_I)=\left(\frac{S^2\tau_g}{1+i^2\omega_I^2\tau_g^2}+\frac{(1-S^2)\tau}{1+i^2\omega_I^2\tau^2}\right) \qquad i=1,2 \tag{18}$$

The rotational correlation time, τ_{RH} is assumed to have simple exponential temperature dependence with an E_R activation energy as given in Equation (19).

$$\tau_{RH}=\tau_{RH}^{298}exp\left[\frac{E_R}{R}\left(\frac{1}{T}-\frac{1}{298.15}\right)\right] \tag{19}$$

The outer-sphere contribution can be described by Equations (20 and 21) where N_A is the Avogadro constant, and J_{os} is its associated spectral density function as given by Equation (21).[17,18]

$$r_{los}=\frac{32\,N_A\pi}{405}\left(\frac{\mu_0}{4\pi}\right)^2\frac{\hbar^2\gamma_S^2\gamma_I^2}{a_{GdH}D_{GdH}}S(S+1)\left[3J_{os}(\omega_I,T_{1e})+7J_{os}(\omega_S,T_{2e})\right] \tag{20}$$

$$J_{os}(\omega,T_{je})=\mathrm{Re}\left[\frac{1+14\left(i\omega\tau_{GdH}+\frac{\tau_{GdH}}{T_{je}}\right)^{1/2}}{1+\left(i\omega\tau_{GdH}+\frac{\tau_{GdH}}{T_{je}}\right)^{1/2}+49\left(i\omega\tau_{GdH}+\frac{\tau_{GdH}}{T_{je}}\right)+19\left(i\omega\tau_{GdH}+\frac{\tau_{GdH}}{T_{je}}\right)^{3/2}}\right] \tag{21}$$

$j=1,2$

The longitudinal and transverse electronic relaxation rates, $1/T_{1e}$ and $1/T_{2e}$ are expressed by Equations (22 and 23), where τ_v is the electronic correlation time for the modulation of the zero-field-splitting interaction, E_v the corresponding activation energy and Δ^2 is the mean square zero-field-splitting energy. We assumed a simple exponential dependence of τ_v versus $1/T$ as written in Equation (24).

$$\left(\frac{1}{T_{1e}}\right)^{ZFS}=\frac{1}{25}\Delta^2\tau_v\{4S(S+1)-3\}\left(\frac{1}{1+\omega_S^2\tau_v^2}+\frac{4}{1+4\omega_S^2\tau_v^2}\right) \tag{22}$$

$$\left(\frac{1}{T_{2e}}\right)^{ZFS}=\Delta^2\tau_v\left(\frac{5.26}{1+0.372\omega_S^2\tau_v^2}+\frac{7.18}{1+1.24\omega_S\tau_v}\right) \tag{23}$$

$$\tau_v=\tau_v^{298}exp\left[\frac{E_v}{R}\left(\frac{1}{T}-\frac{1}{298.15}\right)\right] \quad (24)$$

The diffusion coefficient for the diffusion of a water proton away from a Gd^{3+} complex, D_{GdH}, is assumed to obey an exponential law versus the inverse of the temperature, with activation energy E_{GdH}, as given in Equation (25). D_{GdH}^{298} is the diffusion coefficient at *298.15* K.

$$D_{GdH}=D_{GdH}^{298}exp\left\{\frac{E_{GdH}}{R}\left(\frac{1}{298.15}-\frac{1}{T}\right)\right\} \quad (25)$$

References

[1] G. Schwarzenbach, H. Flaschka, *Complexometric Titrations*, Methuen, London, **1969**.
[2] N. Thieriet, J. Alsina, E. Giralt, F. Guibe, F. Albericio, *Tetrahedron Lett.* **1997**, *38*, 7275–7278.
[3] A. Beeby, I. M. Clarkson, R. S. Dickins, S. Faulkner, D. Parker, L. Royle, A. S. de Sousa, J. A. G. Williams, M. Woods, *J. Chem. Soc., Perkin Trans. 2* **1999**, 493–504.
[4] A. E. Martell, R. M. Smith, *Critical Stability Constants*, Plenum Press, New York, **1974**.
[5] R. M. Smith, A. E. Martell, R. J. Motekaitis, *Critically Selected Stability Constants of Metal Complexes Database. NIST Standard Reference Database 46*, **2001**.
[6] F. Yerly, *VISUALISEUR 2.3.5*, Switzerland, **1999**.
[7] F. Yerly, *OPTIMISEUR 2.3.5*, Switzerland, **1999**.
[8] P. Caravan, J. J. Ellison, T. J. McMurry, R. B. Lauffer, *Chem. Rev.* **1999**, *99*, 2293–2352.
[9] B. Halle, H. Wennerstrom, *J. Chem. Phys.* **1981**, *75*, 1928–1943.
[10] É. Tóth, D. Pubanz, S. Vauthey, L. Helm, A. E. Merbach, *Chem.-Eur. J.* **1996**, *2*, 1607–1615.
[11] D. Raiford, C. Fisk, E. Becker, *Anal. Chem.* **1979**, *51*, 2050–2051.
[12] S. Meiboom, D. Gill, *Rev. Sci. Instrum.* **1958**, *29*, 688–691.
[13] K. Micskei, L. Helm, E. Brucher, A. Merbach, *Inorg. Chem.* **1993**, *32*, 3844–3850.
[14] A. Hugi, L. Helm, A. Merbach, *Helv. Chim. Acta* **1985**, *68*, 508–521.
[15] Z. Luz, S. Meiboom, *J. Chem. Phys.* **1964**, *40*, 2686–2692.
[16] F. A. Dunand, E. Toth, R. Hollister, A. E. Merbach, *J. Biol. Inorg. Chem.* **2001**, *6*, 247–255.
[17] J. Freed, *J. Chem. Phys.* **1978**, *68*, 4034–4037.
[18] S. Koenig, R. Brown, M. Spiller, B. Chakrabarti, A. Pande, *Biophys. J.* **1992**, *61*, 776–785.